

A review of the fall/winter 2000/01 and comparison with 1978/79.

J. Cohen, AER Inc., jcohen@aer.com

A review of fall/winter 2000/01 shows it consistent with the hypothesis that the winter Arctic Oscillation (AO) is characterized by the westward and northward expansion of the Siberian high. However comparison with the fall/winter of 1978/79, chosen because the winter AO is of comparable sign and magnitude, demonstrates that the westward and northward expansion of the Siberian high cannot explain all winters. Instead a novel and more comprehensive framework is presented to explain the evolution of the AO which is the dominant winter mode. It is shown that there exists a dichotomy of pathways with the characteristics of the dominant mode dependent upon the pathway taken. All winters examined fall into one of the two different dynamic evolutions presented, the knowledge of which clarifies prior uncertainties associated with the dominant mode and provides excellent potential for the successful prediction of subsequent winter mean climate states.

Introduction

The AO is characterized by a strong oscillation in a pressure/height center anomaly covering the entire Arctic basin, extending from the surface well into the stratosphere. At mid-latitudes an opposite pressure height anomaly stretches mostly across the two major ocean basins (Thompson and Wallace 1998). This dominant mode of winter Northern Hemisphere (NH) atmospheric pressure variability has been linked with variability in sea surface temperatures, snow cover, sea ice, stratospheric forcing and aerosols (Rodwell et al. 1999; Cohen and Entekhabi 1999; Mysak and Venegas 1998; Baldwin and Dunkerton 1999; Shindell et al. 1999). Furthermore this mode has been shown to originate in the lower troposphere in eastern Eurasia in October (Cohen et al. 2001), in contrast with the demonstrated downward propagation of the mode from the stratosphere sometime after the beginning of November (Baldwin and Dunkerton 1999). We analyze daily data (NCEP/NCAR reanalysis data; Kalnay et al. 1996) from two winters where strong negative AO signals were observed (about one standard deviation below normal). To emphasize dynamical characteristics rather than statistical ones, we will present results from two paradigm winters (1978/79, 2000/01) and list other years that bear resemblance to these two paradigm years. We will then conclude with a composite analysis, which will demonstrate the generality of these two winters.

Results

We analyze pressure/height fields for horizontal and vertical propagation of anomalies influential in characterizing the dominant NH winter mode. We begin our analysis with multi-day averaged sea level pressure (SLP) anomalies starting with September 22, 2000 in Figure 1. The propagation and growth of the SLP anomaly is similar to a composited analysis for 1972-1998 (Cohen et al. 2001) and consistent with the hypothesis that the winter AO signal originates in the lower troposphere in eastern Siberia during fall and is forced by snow cover variations (in fall 2000 Siberian snow cover was above normal; Robinson et al. 1993). The original SLP anomaly first propagates to the west and then northward across the Arctic where at its peak it closely resembles the canonical AO pattern. From calculation of the daily AO with height (Baldwin and Dunkerton 1999), the AO pattern appears to originate in the stratosphere and propagate down into the troposphere on a time scale of about two weeks during December (not shown). Therefore the winter of 2000/01 is a good example of the contradiction posed earlier, i.e., how could the AO both originate in the lower troposphere and mid-upper stratosphere?

We substitute the AO diagnostic with one that is designed to capture both the hemispheric scale AO pattern of the stratosphere and troposphere, and the more regional precursor height anomaly, which originates near the surface. Because the most prominent feature of the AO pattern is a coherent and same-signed height anomaly of all regions north of 60°N (Thompson and Wallace 1998), we plot the area averaged normalized height anomaly summed over every grid box of that polar cap (Figure 2a). The diagnostic is an excellent proxy for the AO, yet by eliminating all areas south of 60°N it also captures the dominant regional height anomaly at high latitudes. The downward propagation of the height anomaly corresponds well with the one shown by computing the AO. But it also clearly shows that the downward propagating anomaly indeed originated even earlier near the surface. The diagnostic nicely shows that the winter AO originated in the troposphere propagated upwards into the stratosphere and was then reflected back into the troposphere. These results are consistent for all strong AO events examined since 1968 that also show a downward propagating AO signal from the stratosphere into the troposphere.

Siberia is the major source of vertical wave activity flux (WAF) for the Northern Hemisphere (Plumb 1985). The most important contribution to the variation in interannual WAF is diabatic heating, with radiational cooling enhancing the upward WAF and heating reducing the upward WAF (Ringler and Cook 1999). It has already been shown that preceding the downward propagation of the zonal wind anomalies from the stratosphere to the troposphere, associated with the winter AO, is anomalous upward WAF in the fall over Siberia (Saito et al. 2001). Vertical propagation of anomalous wave energy is forced by planetary-scale Rossby waves (Plumb 1985). Consistent with this result, calculations of WAF anomalies (Plumb 1985) for October and November 2000, shown in Panels 2b and 2c, show strong upward flux of energy originating in the lower troposphere and eventually propagating throughout the troposphere and much of the stratosphere. The zonal component of the WAF shows the center of greatest flux to emanate from the region of the large SLP anomaly in Eurasia (not shown). While in December the WAF reverses and is downward in the lower stratosphere and troposphere

(Panel 2d). Greater absorption of WAF in the stratosphere results in negative zonal wind anomalies, which then propagate downward as occurred in December 2000 (not shown). Positive fall SLP and lower tropospheric height anomalies supported or maintained by positive snow anomalies, are the precursors of the downward propagation of the negative winter AO signal observed. In autumns of large negative height anomalies and reduced snow cover, the upwards WAF is decreased, zonal winds in the stratosphere accelerate and downward propagation of positive zonal wind anomalies commence in the early winter.

The troposphere has many more degrees of freedom than the stratosphere (Perlwitz and Graf 2001). Lower tropospheric boundaries are constrained by the existing boundary conditions and mostly remain regionalized. On the other hand, these boundaries do not exist in the stratosphere where anomalies can spread quickly and become hemispheric in scale. We propose that, in winters similar to 2000/01, the winter AO originates regionally in Eurasia and that energy from this regional anomaly propagates vertically into the stratosphere where it spreads out. Since the pattern of variability tends to be annular in the stratosphere (Cohen and Saito 2002), the descending signal from the stratosphere to the troposphere is most likely to be annular. However as it turns out the annular mechanism is the exception rather than the rule for the formation of the winter AO.

In Figure 2 we also plot the same vertical anomaly propagation diagnostics for the fall/winter of 1978/79. This time both the AO diagnostic (not shown) and the normalized height anomalies (Panel 2e), both demonstrate that the tropospheric AO anomaly is decoupled from the stratosphere. Calculations of WAF (Panels 2f-2h) and zonal wind anomalies (not shown) show little in the way of enhanced vertical propagation. In Figure 3 we plot the multi-day averaged SLP anomalies from October 1, 1978 - January 31, 1979. The SLP anomaly that eventually resulted in the dominant SLP pattern for the winter propagated eastward from the North Atlantic Ocean into Eurasia. Since the SLP anomaly, which eventually formed the dominant winter AO pattern, was located in the North Atlantic region during the fall remote from Siberia, it is therefore unlikely to influence significantly the vertical WAF. Once winter begins the troposphere and stratosphere are decoupled (Charney and Drazin 1961; Kodera and Kuroda 2000), the AO anomaly is trapped in the troposphere and cannot communicate with the stratosphere. This isolation leads to a slower evolution and a more regional anomaly pattern. The resultant anomaly pattern rather than being annular, more closely resembles the pattern of variability associated with the NAO.

Discussion

We analyzed the evolution of SLP/height anomalies of every winter since 1972/1973 and also included the two strong AO winters of 1965/66 and 1968/69. Winters were then categorized (N or A) according to similarity with the paradigm winters of 1978/79 and 2000/01. In the more common type, the SLP anomaly propagates upstream from the North Atlantic or North America into Eurasia, and because the antecedent anomaly originates remote from Siberia it does not influence the stratosphere, is therefore trapped in the troposphere during the winter months, evolution is slower, and the pattern is more

regionalized. The resultant pattern is more likely to resemble the NAO pattern of variability (Type N), and the associated climate anomalies are more likely to be focused in western Eurasia and the North Atlantic. In the second type, the SLP anomaly propagates downstream from eastern Siberia into central Eurasia (in some years this anomaly combines with an already existing anomaly to the west, as happened in the fall of 2000). Because the anomaly forms in Siberia it is most likely to propagate vertically from the troposphere into the stratosphere, which results in a downward propagation of energy from the stratosphere.. As the anomaly descends from the stratosphere to the troposphere the SLP anomaly is quickly pulled across the polar cap into North America. This AO or annular pattern of variability (Type A), and the associated climate anomalies are more likely to be focused in eastern Eurasia and eastern North America.

In Table 1 we list all winters analyzed according to type and highlight strong positive and negative phases in each category with a plus or minus sign accordingly. From Table 1 it is apparent that Type N occurs in greater frequency. Yet since 1972 the stronger events have been overwhelmingly Type A. Also there has been a definite trend of less Type N and more Type A strong events since 1960; there has not been a strong Type N event since 1985. We calculate in Figure 4 the first EOF of monthly SLP since 1960 grouped solely by Type N (Panel 4a) and Type A (Panel 4b), with no other manipulation of the data. The pattern of variability in Type N years is most closely associated with that of the NAO; involving signals in the North Atlantic and western Eurasia with little in the Pacific or annularity. The pattern of variability for Type A years is most closely associated with that of the AO, where the variability in the North Pacific closely resembles the one in the North Atlantic, giving the appearance of zonal symmetry or annularity.

Finally in Figure 4c we create an index using Siberian snow cover and NH SLP anomalies from October (Cohen et al. 2001) and correlate it with the following DJF AO. SLP anomalies were chosen from eastern Eurasia preceding a Type N event and from the North Atlantic and North America preceding a Type A event. The correlation between the two indices is 0.93. Forecasting a Type N or Type A appears relatively simple. The default is the more common Type N. Type A events require an organized SLP anomaly in eastern Siberia, which propagates westward. Figure 4c suggests that forecasting mean NH winter conditions may be no more difficult than short-range weather forecasting, with comparable skill.

Conclusion

As has been shown in other Climate Diagnostic Workshop presentations, the October SLP/snow index is plotted with a sample of observed winter temperatures from three eastern U.S. cities in Figure 5. The correlation between the snow/SLP index is correlated with all three station temperatures at greater than 0.6; demonstrating excellent potential for wintertime climate prediction.

Until now predictability of the NAO/AO has been poor due to the blending of two different dynamical evolutions. Recognizing their distinctive dynamical frameworks will lead to better understanding of past and forecasts of future winter states.

References

- Baldwin, M. P., and T. J. Dunkerton, 1999: Propagation of the Arctic Oscillation from the stratosphere to the troposphere. *J. Geophys. Res.*, **104**, 30,937-30,946.
- Cohen, J. and D. Entekhabi, 1999: Eurasian snow cover variability and Northern Hemisphere climate predictability. *Geophys. Res. Lett.*, **26**, 345-348.
- Cohen, J., K. Saito and D. Entekhabi, 2001: The role of the Siberian high in Northern Hemisphere climate variability. *Geophys. Res. Lett.*, **28**, 299-302.
- Cohen, J. and K. Saito, 2002: A test for annular modes. *J. Climate*, in review.
- Kalnay, E. and Coauthors, 1996: The NCEP/NCAR 40-Year reanalysis project. *Bull. Amer. Meteor. Soc.*, **77**, 437-471.
- Kodera, K. and Y. Kuroda, 2000: Tropospheric and stratospheric aspects of the Arctic Oscillation. *Geophys. Res. Lett.*, **27**, 3349-3352.
- Mysak, L.A. and S.A. Venegas, 1998: Decadal climate oscillations in the Arctic: A new feedback loop for atmosphere-ice-ocean interactions. *Geophys. Res. Lett.*, **25**, 3607-3610.
- Perlwitz, J. and H.-F. Graf, 2001: The variability of the horizontal circulation in the troposphere and stratosphere - A comparison. *Theoret. Appl. Climatol.*, in press.
- Plumb, R.A., 1985: On the three-dimensional propagation of stationary waves. *J. Atmos. Sci.*, **42**, 217-229.
- Ringler, T.D. and K.H. Cook, 1999: Understanding the seasonality of orographically forced stationary waves: Interactions between mechanical and thermal forcing. *J. Atmos. Sci.*, **56**, 1154-1174.
- Robinson, D. A., F. Dewey, and R. Heim Jr., 1993: Northern Hemispheric snow cover: An update. *Bull. Amer. Meteor. Soc.*, **74**, 1689-1696.
- Rodwell, M.J., D.P. Rowell and C.K. Folland, 1999: Oceanic forcing of the wintertime North Atlantic Oscillation and European climate. *Nature*, **398**, 320-323.
- Saito, K., J. Cohen and D. Entekhabi, 2001: Evolution of atmospheric response to early-season Eurasian snow cover anomalies. *Mon. Wea. Rev.*, **129**, 2746-2760.

Shindell, D.T., R.L. Miller, G. Schmidt, and L. Pandolfo, 1999: Simulation of recent northern hemisphere climate trends by greenhouse gas forcing. *Nature*, **398**, 452-455.

Thompson, D. W. J. and J. M. Wallace, 1998: The Arctic Oscillation signature in the wintertime geopotential height and temperature fields. *Geophys. Res. Lett.*, **25**, 1297-1300.

Table 1. List of Type N and Type A events of Arctic Oscillation DJFs during 1972/73-2000/01. Also included are two strong events from the 1960's - 1965/66 and 1968/69. DJF listed under same year as December (e.g., DJF 1972/73 listed under calendar year 1972). Type N and Type A events are described in text. Strong events (+/- one standard deviation) are denoted by +/- depending on phase. Some events which displayed elements of both type of events are denoted with an asterisk.

Dynamic Type of Arctic Oscillation	Years
Type N events:	1965-, 1968-, 1972+, 1973, 1974, 1977, 1978-, 1980, 1981, 1982, 1983*, 1985-, 1986, 1987, 1989*, 1990*, 1993, 1994*, 1995*, 1996*, 1997, 1998*, 1999
Type A events:	1975+, 1976-, 1979, 1984-, 1988+, 1991+, 1992+, 2000-

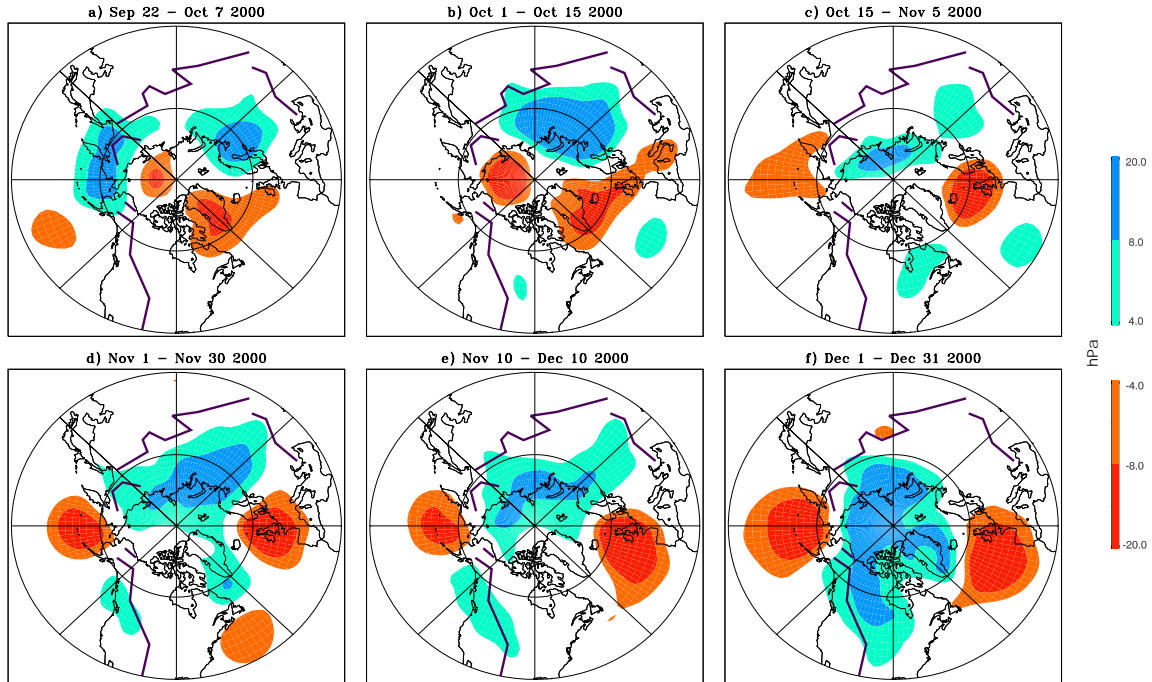


Figure 1: Maps of 15-31 daily averaged NH gridded sea level pressure anomalies for (a) Sep 22 - Oct 7 2000 (b) Oct 1 - Oct 15 2000 (c) Oct 15 - Nov 5 2000 (d) Nov 1 - Nov 30 2000 (e) Nov 10 - Dec 10 2000 (f) Dec 1 - Dec 31 2000. Solid purple lines in a-e are 1000 meter isopleth. Light blue shading for anomalies ≥ 4 hPa and dark blue for anomalies ≥ 8 hPa. Orange shading for anomalies ≤ -4 hPa and red for anomalies ≤ -8 hPa.

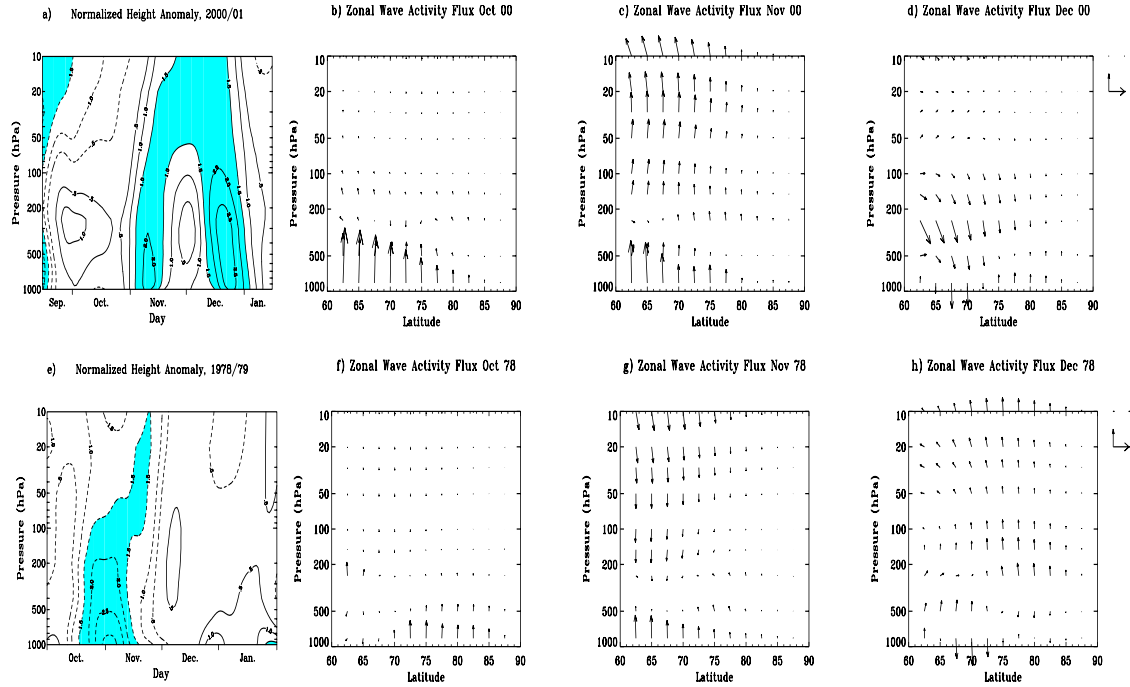


Figure 2: a) Daily value of area-averaged normalized height anomaly for all grid points north of $60^{\circ}N$ from Sep 15 2000 - Jan 15 2001 (28-day filter was applied). Values greater than 1.5 and less than -1.5 are shaded blue. Note strong positive anomaly first propagates upward beginning of November and is reflected down from stratosphere beginning in December. b) Zonal mean of wave activity flux anomaly for October 2000. c) same as b) except for November 2000. d) same as b) except for December 2000. In b) c) and d) value of reference arrows to right are 3.0 (meridional component) and 9.0×10^{-2} (vertical component) m^2/s^2 , all values are scaled by $(pressure/150)^{1/2}$. Note strong upward flux of energy beginning in the lower troposphere in October which extends into the stratosphere in November and is then downward in December. e) Same as a) except for Oct 1 1978 - Jan 31 1979. f) same as b) except for October 1978. g) same as c) except for November 1978. h) same as d) except for December 1978. Note in e)-h) no organized upward propagation of height anomalies or wave activity flux is observed from the troposphere into the stratosphere or vice versa.

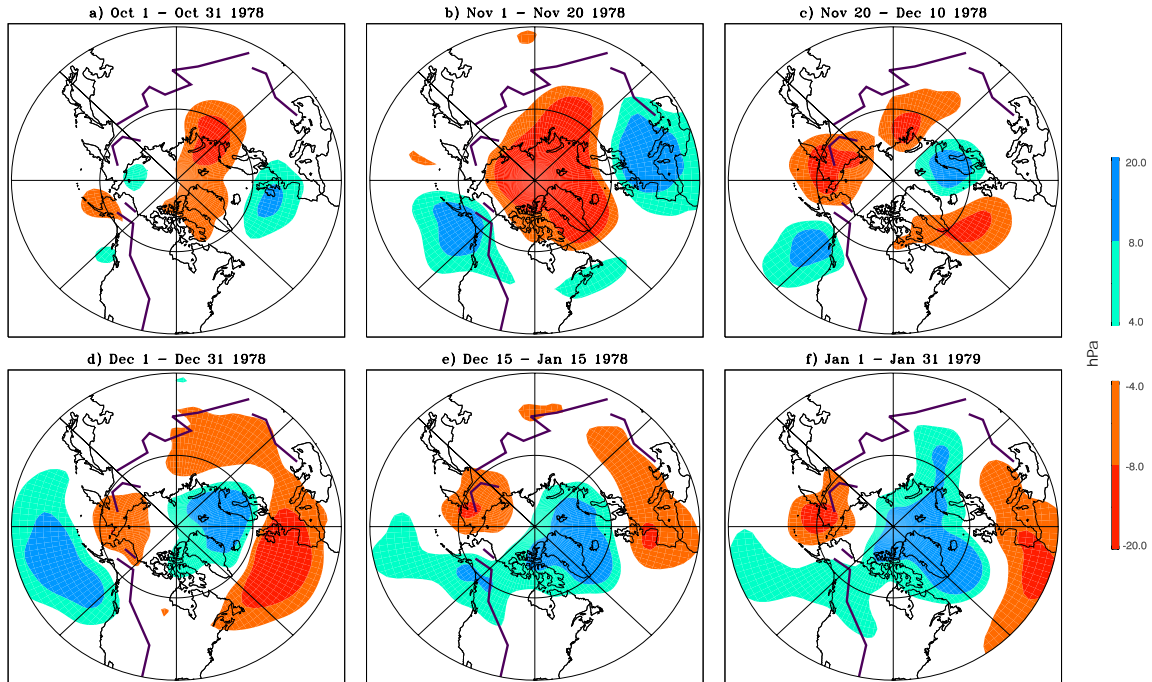


Figure 3: Maps of 20-31 daily averaged NH gridded SLP anomalies for (a) Oct 1 - Oct 31 1978 (b) Nov 1 - Nov 20 1978 (c) Nov 20 - Dec 10 1978 (d) Dec 1 - Dec 31 1978 (e) Dec 15 - Jan 15 1978/79 (f) Jan 1 - Jan 31 1979. Solid purple thick lines in a-e are 1000 meter isopleth. Light blue shading for anomalies ≥ 4 hPa and dark blue for anomalies ≥ 8 hPa. Orange shading for anomalies ≤ -4 hPa and red for anomalies ≤ -8 hPa.

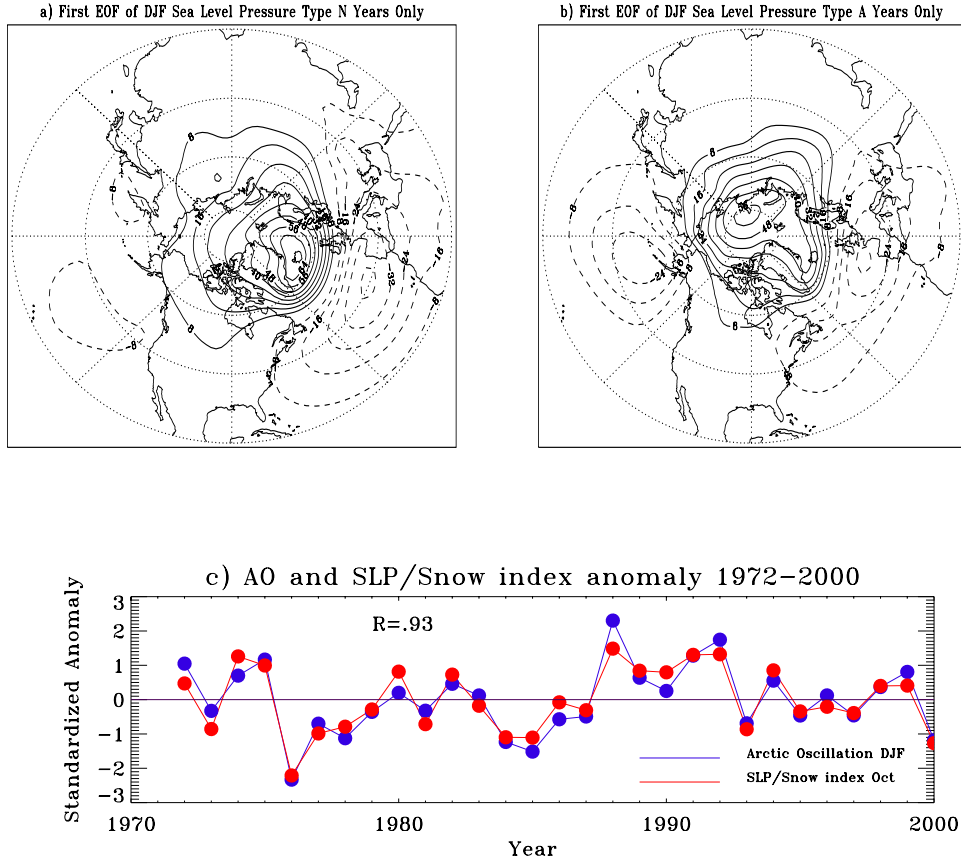


Figure 4: The leading mode of December, January and February monthly sea level pressure variability for a) all winter months from the years listed in Table 1 as Type N (including all winter months from December 1960 thru February 1972) and b) all winter months from the years listed in Table 1 as Type A. c) Standardized DJF time series of the principal component of the leading mode of sea level pressure variability for all winters since 1972/73 (DJF AO, in blue) and a sea level pressure/snow index derived from the linear combination of October sea level pressure anomalies and snow cover area anomalies (Oct SLP/Snow index in red). Correlation between two time series is also shown.

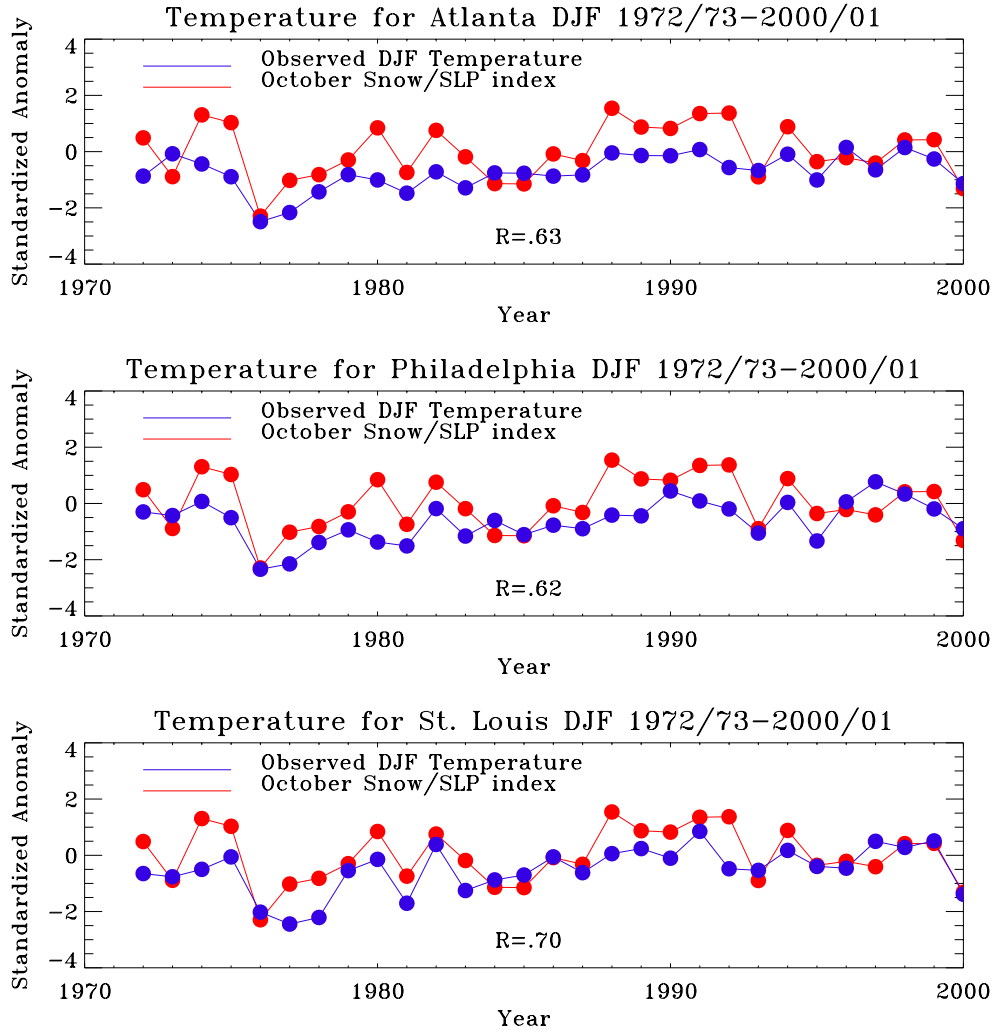


Figure 5: a) Observed surface temperatures for DJF and SLP/snow index for October for Atlanta 1972-2000. b) Observed surface temperatures for DJF and SLP/snow index for October for Philadelphia 1972-2000. c) Observed surface temperatures for DJF and SLP/snow index for October for St. Louis 1972-2000. Included in all three plots is correlation between both time series.